UCRL-10436

University of California

Ernest O. Lawrence Radiation Laboratory

TWO-WEEK LOAN COPY

This is a Library Circulating Copy
which may be borrowed for two weeks.
For a personal retention copy, call
Tech. Info. Division, Ext. 5545

Berkeley, California

UCRL-10436
c.2

DISCLAIMER

This document was prepared as an account of work sponsored by the United States Government. While this document is believed to contain correct information, neither the United States Government nor any agency thereof, nor the Regents of the University of California, nor any of their employees, makes any warranty, express or implied, or assumes any legal responsibility for the accuracy, completeness, or usefulness of any information, apparatus, product, or process disclosed, or represents that its use would not infringe privately owned rights. Reference herein to any specific commercial product, process, or service by its trade name, trademark, manufacturer, or otherwise, does not necessarily constitute or imply its endorsement, recommendation, or favoring by the United States Government or any agency thereof, or the Regents of the University of California. The views and opinions of authors expressed herein do not necessarily state or reflect those of the United States Government or any agency thereof or the Regents of the University of California.

For Phys. Rev.

UCRL-10436

UNIVERSITY OF CALIFORNIA

Lawrence Radiation Laboratory
Berkeley, California

Contract No. W-7405-eng-48

PION-NUCLEON ELASTIC SCATTERING AT 310 MeV: PHASE-SHIFT ANALYSIS

Olav T. Vik and Hugo R. Rugge

August 14, 1962

PION-NUCLEON ELASTIC SCATTERING AT 310 MeV: PHASE-SHIFT ANALYSIS

Olav T. Vik and Hugo R. Rugge

Lawrence Radiation Laboratory
University of California
Berkeley, California

August 14, 1962

ABSTRACT

A phase-shift analysis of π^+-p and π^--p elastic scattering at 310 MeV has been performed. The data includes differential and total cross-section and recoil-proton polarization data for both π^+-p and π^--p elastic scattering, as well as differential cross section data for charge-exchange scattering. Inclusion of d waves was necessary to attain an adequate fit to the data; in the case of π^--p differential cross section, the best fit included f waves. A general phase-shift search using s, p and d waves was carried out; a single solution was obtained that adequately fit all the available data. The most notable characteristics of this solution are I-spin 3/2 phase shifts similar to those obtained in a previous analysis of the π^+-p data and a relatively large $D_{1,5}$ phase shift equal to approximately 15 deg. Errors on the I-spin 1/2 phase shifts of this solution range from 0.3 to 0.9 deg. The I-spin 3/2 phase-shift errors are similar to those obtained previously. Because the π^--p differential cross-section data indicated a possible need for f waves, and since the only satisfactory spd solution displayed a large d-wave phase shift in the I-spin 1/2 state, the analysis was extended to include f waves. The result of allowing f waves was to increase the errors on each of the phase shifts (up to about 2 deg), and also to introduce two new solutions, neither of which can be ruled out statistically. These new solutions

are similar to the d-wave solution in the I-spin 3/2 phase shifts, but vary rather widely in I-spin 1/2 phase shifts. Inelastic scattering processes were neglected throughout most of the analysis; however, a study of their effects on the final solutions was made and these effects were seen to be unimportant.

PION-NUCLEON ELASTIC SCATTERING AT 310 MeV: PHASE-SHIFT ANALYSIS*

Olav T. Vik† and Hugo R. Rugge‡

Lawrence Radiation Laboratory
University of California
Berkeley, California

August 14, 1962

I. INTRODUCTION

A series of experiments on π^--p elastic scattering at an incident-pion kinetic energy of 310 MeV have been completed. These measurements complement the π^+-p elastic scattering data obtained by Rogers et al.[1] and Foote et al.[2] The relatively high accuracy of all of this data makes it practical to perform an accurate phase-shift analysis. The data used in this analysis is the following: for π^--p $\rightarrow$ π^--p, the differential cross section (DCS) measured at 28 angles,[3] the total cross section,[4] and the recoil-proton polarization measured at 4 angles;[3] For π^+-p $\rightarrow$ π^+-p, the differential cross section measured at 23 angles,[1] the total cross section,[1] and the recoil-proton polarization measured at 4 angles.[2] Also incorporated is a charge-exchange differential cross-section measurement at 317 MeV by Caris et al.,[5] and an approximate inelastic cross-section determination by Barish et al.[6]

Analysis of scattering data can be carried out in terms of partial-wave expansions and phase shifts. These phase shifts have been the usual meeting place of theory and experiment for elastic scattering. Sufficiently accurate scattering data can lead to a rather precise determination of the phase shifts, which in turn can impose limitations on any proposed theory of the pion-nucleon interaction.

Analysis of π^--p scattering provides information about both the I-spin 1/2 and I-spin 3/2 states of the π-N system, whereas analysis of π^+-p scattering gives information only about the I-spin 3/2 state. While the I-spin 3/2 phase shifts

are fairly well known, most of the I-spin 1/2 shifts are uncertain in magnitude and even in sign. The uncertainty in the energy region below 300 MeV is mostly due to the fact that the I=3/2 shifts dominate the interaction to such an extent that they effectively mask the contributions of the I-spin 1/2 phase shifts to the experimentally measurable quantities. An accurate phase-shift analysis of the π^+-p data at 310 MeV has already been completed by Foote et al.,[7] so it is mainly the purpose of this data to provide information about the I-spin 1/2 phase shifts at 310 MeV, as well as to yield a better determination of the I-spin 3/2 shifts.

An analysis of the π^--p DCS data, as well as the previous π^+-p analysis, indicated that at least d(up to and including $\ell = 2$) waves must be employed to fit the experimental data well. Furthermore, the best fit to the π^--p data was obtained by including f(up to $\ell = 3$) waves. For this reason an spd analysis and an spdf analysis of the data has been made. Section II presents the equations used in the analysis. In Section III we describe the search program, and in Section IV the phase-shift investigations and results of these investigations. A discussion of results follows in Section V.

II. PHASE-SHIFT EQUATIONS

This section outlines the connection between the observable quantities that can be measured and the π-N phase shifts. The application of the usual phase-shift equations to systems of $\pi^{\pm}$-p and π^{0}-n is reviewed, and finally the equations including nonrelativistic Coulomb and first-order relativistic Coulomb corrections are presented.

A. Cross-Section and Polarization Expressions

The notation used in this section is essentially that used in Bethe and Morrison.[8] In terms of $g(\theta)$ and $h(\theta)$, the non-spin-flip and spin-flip scattering amplitudes, the differential cross section (hereafter referred to as DCS) is expressed by

$$\frac{d\sigma}{d\Omega}(\theta) = \left| g(\theta)\right|^2 + \left| h(\theta)\right|^2 . \qquad (1)$$

The expression for polarization of a proton scattered from a pion is

$$P(\theta) = 2\,\frac{\mathrm{Re}\left[g^*(\theta)\,h(\theta)\right]}{\frac{d\sigma}{d\Omega}(\theta)} . \qquad (2)$$

B. Scattering Amplitudes

1. Non-Spin-Flip and Spin-Flip Amplitudes

The derivation of the partial-wave expansions of the scattering amplitudes is carried out in many references, as for example, Ashkin.[9] Neglecting Coulomb effects, the result for the non-spin-flip amplitude is

$$g(\theta) = \lambda\!\!\!^{-} \sum_{\ell=0}^{\ell_{max}} \left[(\ell+1)\, \frac{\eta_\ell^{+}\exp[2i\delta_\ell^{+}]-1}{2i} + \ell\, \frac{\eta_\ell^{-}\exp[2i\delta_\ell^{-}]-1}{2i} \right] P_\ell(\cos\theta), \qquad (3)$$

and the spin-flip amplitude is

$$h(\theta) = \lambda\!\!\!^{-} \sum_{\ell=1}^{\ell_{max}} \left[\frac{\eta_\ell^{+}\exp[2i\delta_\ell^{+}]-\eta_\ell^{-}\exp[2i\delta_\ell^{-}]}{2} \right] P_\ell^{1}(\cos\theta). \qquad (4)$$

Definitions of quantities appearing in Eqs. (3) and (4) are

ℓ = orbital-angular-momentum quantum number.

$\delta_\ell^{\pm}$ = phase shifts for orbital-angular-momentum state ℓ and total-angular-momentum quantum number $J = \ell \pm 1/2$.

$\eta_\ell^{\pm}$ = inelastic parameters corresponding to each of the phase shifts. These are ≤ 1, being equal to unity in the absence of inelastic scattering. The use of inelastic parameters allows the phase shift $\delta_\ell^{\pm}$ to be completely real even in the presence of inelastic scattering; in this report the term "phase shift" refers to the real part $\delta_\ell^{\pm}$.

$\lambda\!\!\!^{-}$ = wavelength of either particle in the c.m. system ($\lambda\!\!\!^{-} = 1/k$).

$P_\ell(\cos\theta)$ = Legendre polynomial.

$P_\ell^{1}(\cos\theta)$ = associate Legendre polynomial, defined by

$$P_\ell^{1}(\cos\theta) = \sin\theta \frac{d}{d(\cos\theta)} P_\ell(\cos\theta) .$$

θ = c.m. scattering angle for either the pion or the proton.

2. Isotopic Spin

The π^+-p system, which has a z component of isotopic spin $I_z = 3/2$, can exist only in the isotopic spin state $I = 3/2$. However, the π^--p system, for which $I_z = -1/2$, is a linear combination of isotopic-spin states $I = 3/2$ and $I = 1/2$. As shown, for example, in Bethe and de Hoffman,[10] the scattering amplitudes for the three elastic reactions for charged pions and protons are as shown in Table I.

C. Inclusion of Coulomb Corrections

The scattering amplitudes given by Eqs. (3) and (4) have been extended to take into consideration the nonrelativistic Coulomb effects as well as the first-order relativistic Coulomb corrections. This extension was carried out by Foote et al.[7] and is based on the work of Stapp et al.[11] and Solmitz.[12]

In this section we use Foote's Eqs. (7) and (8) of Section B,[7] to write down Coulomb-corrected scattering amplitudes for the reactions of Table I. It will now be convenient to distinguish between phase shifts for states of isotopic spin 1/2 and 3/2. In our Eqs. (12) through (17) we use the notation:

$\delta_\ell^{\pm}$ = phase shift for orbital-angular-momentum quantum number ℓ, total-angular-momentum state $J = \ell \pm 1/2$, and isotopic-spin state $I = 1/2$;

$\eta_\ell^{\pm}$ = inelastic parameter (defined in Section II-B-1) corresponding to the $\delta_\ell^{\pm}$ phase shift above;

$\alpha_\ell^{\pm}$ = phase shift for orbital-angular-momentum quantum number ℓ, total-angular-momentum state $J = \ell \pm 1/2$, and isotopic-spin state $I = 3/2$;

$\rho_\ell^{\pm}$ = inelastic parameter corresponding to the $\alpha_\ell^{\pm}$ phase shift above.

The new quantities to be introduced in Eqs. (12) through (17) are

$$n = \frac{e^2}{hv} , \tag{5}$$

where v is the laboratory-system velocity of the incident pion, and

$$B = \frac{(\mu_p \beta_p \beta_\pi)/2 + (2\mu_p - 1)\beta_p^2/4}{1 + \beta_\pi \beta_p} , \tag{6}$$

where μ_p = magnetic moment of the proton in nuclear magnetons, and β_p, β_π = c. m. velocities of the proton and pion divided by the velocity of light.

The $\overline{\Phi}_\ell$ is the nonrelativistic Coulomb phase shift of order ℓ. It is equal to 0 for $\ell = 0$, and is given by

$$\overline{\Phi}_\ell = \sum_{x=1}^{\ell} \tan^{-1} \left(\frac{n}{x}\right), \text{ for } \ell \geq 1. \tag{7}$$

The additional parenthetical (+, -, or 0) that appears on the phase shifts in Eqs. (12) through (17) is necessitated because the phase shifts used in those expressions are <u>total</u> phase shifts, differing from the nuclear shifts by a small term $\overline{\Phi}_\ell^{\pm}$, which is the complete Coulomb phase shift of order ℓ. This is explained below.

The total phase shifts are related to the nuclear shifts by

$$a_\ell^{\pm}(+) = a_\ell^{\pm} + \overline{\Phi}_\ell^{\pm} , \qquad a_\ell^{\pm}(0) = a_\ell^{\pm} - \overline{\Phi}_\ell^{\pm}/2,$$

$$a_\ell^{\pm}(-) = a_\ell^{\pm} - \overline{\Phi}_\ell^{\pm} , \qquad \delta_\ell^{\pm}(0) = \delta_\ell^{\pm} - \overline{\Phi}_\ell^{\pm}/2 .$$

$$\delta_\ell^{\pm}(-) = \delta_\ell^{\pm} - \overline{\Phi}_\ell^{\pm} .$$

The complete Coulomb phase shift of order ℓ, $\overline{\Phi}_\ell^{\pm}$, consists of the nonrelativistic Coulomb phase shift defined by Eq. (2.11), plus a first-order relativistic correction,

$$\overline{\Phi}_\ell^{\pm} = \overline{\Phi}_\ell + \Delta\overline{\Phi}_\ell^{\pm} , \tag{8}$$

where the first-order relativistic Coulomb term is given by

$$\Delta\overline{\Phi}_0 \approx n \left[\frac{1}{2} (\beta_p \beta_\pi) + \frac{1}{4} (2\mu_p - 1)\beta_p^2/(1 + \beta_\pi \beta_p) \right] ; \tag{9}$$

$$\Delta\overline{\Phi}_\ell^{\,+} \approx n\, B/(\ell + 1) \text{ for } \ell \geq 1, \tag{10}$$

and

$$\Delta\overline{\Phi}_\ell^{\,-} \approx - \frac{nB}{\ell} , \text{ for } \ell \geq 1 . \tag{11}$$

The above Coulomb phase shifts for incident pion kinetic energy $T_\pi = 310$ MeV are given in Table II.

The Coulomb-corrected scattering amplitudes for the reactions of Table I are:

<u>Reaction (a), $\pi^+ + p \rightarrow \pi^+ + p$:</u>

$$g(\theta) = - \frac{kn}{2 \sin^2\theta/2} \exp\left\{ -i\, n\, \ln[\sin^2(\theta/2)] \right\}$$

$$+ k \sum_{\ell = 0}^{\ell_{max}} \left\{ (\ell + 1) \frac{\rho_\ell^{\,+} \exp[2 i\, a_\ell^{\,+}(+)] - \exp[2i\overline{\Phi}_\ell]}{2i} \right.$$

$$\left. + \ell \frac{\rho_\ell^{\,-} \exp[2ia_\ell^{\,-}(+)] - \exp[2i\overline{\Phi}_\ell]}{2i} \right\} P_\ell(\cos\theta) , \tag{12}$$

and

$$h(\theta) = \frac{ikn\, B \sin\theta}{2 \sin^2\theta/2} + k \sum_{\ell = 1}^{\ell_{max}} \left[\frac{\rho_\ell^{\,+} \exp[2ia_\ell^{\,+}(+)] - \rho_\ell^{\,-} \exp[2i\, a_\ell^{\,-}(+)]}{2} \right.$$

$$\left. - i\, n\, B \frac{2\ell+1}{\ell(\ell+1)} \right] P_\ell^{\,1}(\cos\theta) . \tag{13}$$

Reaction (b), $\pi^- + p \to \pi^- + p$:

$$g(\theta) = \frac{kn}{2\sin^2\theta/2} \exp\, i\, n\, \ln \sin^2(\theta/2)$$

$$+ k \sum_{\ell=0}^{\ell_{max}} \left[(\ell+1) \frac{\rho_\ell^+ \exp[2i\alpha_\ell^+(-)] + 2\eta_\ell^+ \exp[2i\delta_\ell^+(-)]}{6i} \right.$$

$$+ \ell \frac{\rho_\ell^- \exp[2i\alpha_\ell^-(-)] + 2\eta_\ell^- \exp[2i\delta_\ell^-(-)]}{6i}$$

$$\left. - (2\ell+1) \frac{\exp[-2i\bar{\Phi}_\ell]}{2i} \right] P_\ell(\cos\theta), \tag{14}$$

and

$$h(\theta) = \frac{ikn\, B \sin\theta}{2\sin^2\theta/2}$$

$$+ \sum_{\ell=1}^{\ell_{max}} \left[\frac{\rho_\ell^+ \exp[2i\alpha_\ell^+(-)] + 2\eta_\ell^+ \exp[2i\delta_\ell^+(-)] - \rho_\ell^+ \exp[2i\alpha_\ell^-(-)]}{6} \right.$$

$$- \frac{2\eta_\ell^- \exp[2i\delta_\ell^-(\delta)]}{6} \tag{15}$$

$$\left. + i\, n\, B \left(\frac{2\ell+1}{\ell(\ell+1)} \right) \right] P_\ell^1(\cos\theta).$$

Reaction (c), $\pi^- + p \to \pi^0 + n$:

In this reaction, the incoming particles are charged and the outgoing particles are neutral. One may therefore, to the accuracy desired in this analysis, consider the Coulomb perturbation to be half as great as in reaction (b). Hence, when we use the proper isotopic-spin decomposition shown in Table I, the scattering amplitudes are given by

$$g(\theta) = \frac{\sqrt{2}}{3} k \sum_{\ell=0}^{\ell_{max}} \left[(\ell+1) \frac{\rho_\ell^+ \exp[2i\alpha_\ell^+(0)] - \eta_\ell^+ \exp[2i\delta_\ell^+(0)]}{2i} \right.$$

$$\left. + \ell \frac{\rho_\ell^- \exp[2i\alpha_\ell^-(0)] - \eta_\ell^- \exp[2i\alpha_\ell^-(0)]}{2i} \right] P_\ell(\cos\theta), \tag{16}$$

and

$$h(\theta) = \frac{\sqrt{2}}{3} k \sum_{\ell=1}^{\ell_{max}} \left[\frac{\rho_\ell^+ \exp[2i\alpha_\ell^+(0)] - \eta_\ell^+ \exp[2i\delta_\ell^+(0)] - \rho_\ell^- \exp[2i\alpha_\ell^-(0)]}{2} \right.$$

$$\left. + \frac{\eta_\ell^- \exp[2i\delta_\ell^-(0)]}{2} \right] P_\ell^1(\cos\theta). \tag{17}$$

D. Phase-Shift Notation

From this point on, "phase shift" will be understood to mean the nuclear part of the total phase shifts used in Eqs. (12) through (17). The notation developed by Foote for the π^+-p system ($I = 3/2$ state)[7] is extended to the $I = 3/2$ and $I = 1/2$ isotopic-spin states. The symbol itself denotes the orbital-angular-momentum state (s, p, d, etc.), the first subscript denotes twice the isotopic spin, and the second subscript denotes twice the total angular momentum (i.e., $\ell_{2I,\,2J}$). The symbols are summarized in Table III.

III. SEARCH PROGRAM

Several IBM 7090 programs have been written to perform the phase-shift analysis. This section deals with the general methods employed by these programs, and a description of the final program used.

A. General Method

As may be judged from Section II, the phase-shift expansions of the scattering amplitudes describing the π-N system are very complicated functions, and so there is no simple way of deriving values for the phase shifts from the available experimental data. Modern high-speed computer techniques make it possible, however, to calculate very rapidly the values of DCS and polarisation predicted by a given set of phase shifts.

The PIPANAL program, developed for this purpose, employs the grid-search method for fitting the phase-shift equations to experimental points.[13] A tentative set of phase shifts is fed into the program, and the computer then varies all the phase shifts in turn in order to minimize the quantity

$$M = \sum \left[\frac{Q_{calc} - Q_{exp}}{\Delta Q_{exp}} \right]^2 , \tag{18}$$

where Q_{calc} refers to the value of DCS or polarization calculated from a given set of phase shifts, Q_{exp} is the corresponding experimentally determined value, and ΔQ_{exp} is the experimental uncertainty in Q_{exp}. The summation is over all the experimental quantities being considered in a given case.

Each phase shift is varied in turn, and this procedure is repeated until a complete cycle results in no reduction in the value of M. The increment of change in phase shift is then reduced, and the above process is repeated until the increment reaches a certain predetermined value.

B. PIPANAL 1CF4

PIPANAL 1CF4 is based on the IBM 704 program developed by Foote[7] and has evolved through several intermediate programs. It is the most complete program developed, and the only one discussed in this report. It is to be understood, however, that not all the analysis discussed in the following sections was performed by this program, but sometimes by less inclusive and therefore less time-consuming programs of the same type.

1. Experimental Quantities Fitted

Experimental quantities fitted by PIPANAL 1CF4 are:

(a) DCS – The program accepts up to 30 DCS points each for the three reactions given in Table I.

(b) Polarization – The program accepts up to 10 points each for the reactions in Table I.

(c) Total cross section – The program accepts a total cross section for π^+-p and π^--p scattering. Since total cross sections are usually determined experimentally between two cutoff angles, the program fits them to the numerically integrated value under the calculated DCS curve between these cutoff angles. A predetermined fraction of the calculated inelastic cross section was also added, and in the case of π^--p scattering, the integration was under the DCS curve for both reactions (b) and (c) of Table I.

(d) Inelastic cross section – Only the π^--p inelastic cross section was fitted, since only the $I = 1/2$ inelastic parameters are allowed to vary (see Section 2 below).

(e) Legendre coefficients for charge-exchange scattering – The usual way of measuring the DCS for the reactions $\pi^- + p \rightarrow \pi^0 + n$ is to measure the γ-ray distribution from the decaying π^0. When this is the case, the γ-ray distribution is fitted in a Legendre expansion, and the coefficients for a Legendre expansion of the π^0 distribution are related to those of the γ distribution.[14] For this reason, data on the $\pi^- + p \rightarrow \pi^0 + n$ DCS are often quoted in terms of these Legendre coefficients. Therefore the program was equipped to fit these coefficients with coefficients calculated from the phase shifts. Up to seven Legendre coefficients can be fitted (corresponding to an spdf-wave fit to the γ distribution).

2. Variation of Quantities

Quantities varied in SPIPANAL 1CF4 are as follows:

(a) Phase shifts – The program varies phase shifts for $I = 1/2$ and $I = 3/2$ states. It can perform sp, spd, or spdf analysis for $\pi^{\pm}$-p systems of any energy.

(b) Inelastic parameters – In the case of π^+-p scattering, the total inelastic cross section is quite small compared with the total elastic cross section ($\approx$0.5 mb as compared with 60 mb). For this reason, the inelastic parameters $\rho_\ell^{\pm}$ (see Section II-C) are not varied in the search. It is possible, however, to insert $\rho_\ell^{\pm}$ different from 1 into the input data, and thus study the possible effects of inelastic parameters on the phase shifts. The inelastic cross section for π^--p scattering is, however, about 1 mb[6] as compared with $\approx$ 28 mb for the π^--p elastic total cross section. (In this context "elastic" refers to both $\pi^- + p \rightarrow \pi^- + p$ and $\pi^- + p \rightarrow \pi^0 + n$ reactions). We accordingly allowed the quantities $\eta_\ell^{\pm}$ to be varied in the search, with the constraint that they had to remain within the interval $0 \leq \eta_\ell^{\pm} \leq 1$. The assumption made here was that,

since the total inelastic cross section for π^+-p (which is all isotopic spin 3/2) is very small, the contribution to the larger π^--p inelastic cross section must be from the isotopic-spin 1/2 state.

(c) Normalization parameters – In the measurement of DCS there is always an uncertainty of a few percent in the normalization of the angular distributions. So that the search program can move the angular distribution up or down an amount corresponding to this uncertainty, quantities ϵ^+, ϵ^-, and ϵ^0 were introduced for each of the three differential cross sections mentioned in Section III-B-2 above. Each of the experimental DCS points was multiplied by the quantity $(1+\epsilon)$ to adjust the distribution, and the contribution of DCS to Eq. (18) was modified to become

$$M(DCS) = \sum \left\{ \left[\frac{DCS_{calc} - DCS_{exp}(1+\epsilon)}{\Delta\, DCS_{exp}} \right]^2 + \left(\frac{\epsilon}{\Delta\epsilon} \right)^2 \right\}, \tag{19}$$

where $\Delta\epsilon$ is the experimental uncertainty in normalization.

3. Error Routine[15]

The usefulness of any phase-shift solution is limited unless the error on each phase shift is known. Approximate values of the errors on the phase shifts were determined. The method used was the standard error-matrix approach. After the minimum value of M (Eq. 18) has been found, the shape of the M hypersurface near the minimum is examined by computing the second partial derivatives of M with respect to each of the phase shifts used. These partial derivatives form a matrix G defined by

$$G_{ij} = \frac{1}{2} \frac{\partial^2 M}{\partial \delta_i \partial \delta_j} . \tag{20}$$

This matrix is then inverted, yielding the error matrix G^{-1} with the properties

$$\sqrt{(G^{-1})_{ii}} = (\Delta\delta_i)_{rms}, \text{ and } (G^{-1})_{ij} = C_{ij}\,(\Delta\delta_i)_{rms}(\Delta\delta_j)_{rms} (\text{for } i \neq j),$$

where C_{ij} is the correlation coefficient.

IV. PHASE-SHIFT INVESTIGATIONS

The general approach followed in searching for phase-shift solutions to the experimental data is the random-startingpoint method. A large number of sets of random phase shifts (over the range $-180 \text{ deg} \leq \delta \leq 180 \text{ deg}$) are introduced as input data, and the program is requested to find the local minimal value for M. If a sufficient number of randomly located starting points is used, the probability of having missed a "good" solution is small.

When all phase shifts are allowed to vary simultaneously (as in PIPANAL 1CF4) the process of random searching is extremely time-consuming. For this reason, the following method was used: The three (one spd and two spdf) $I = 3/2$ solutions of Foote[7] were taken as starting points and were held fixed in all of the random searching. Only the DCS data of the preceding paper[3] (our Table IV) were fitted in this manner, and for each $I = 3/2$ set, there were in general several $I = 1/2$ sets that satisfactorily fitted the DCS data. These "good" solutions were then inserted into PIPANAL 1CF4, the π^+-p data shown in Tables V and VI were included, and all phase shifts were allowed to vary simultaneously. Polarization data were then introduced (Table VII) and finally charge-exchange DCS (Table VIII) in order to rule out some of the $I = 1/2$ phase-shift sets. This procedure is discussed in detail in the following two subsections.

A. spd Analysis

A least-squares fit of the DCS data of the previous paper[3] indicated the need for at least d waves to obtain a satisfactory fit. This subsection explores the details of the spd analysis.

1. Fermi 3/2 starting point.

In the analysis by Foote (see his Table IV),[7] only the solution of the Fermi type is totally acceptable. The Minami solution is theoretically unsatisfactory because of the very large $D_{3,3}$ shift, and the Yang solution is highly improbable because of the large M value. We therefore concentrated our efforts on the Fermi solution (the Yang type is mentioned briefly below).

Using Foote's Fermi solution ($S_{3,1} = -18.5$; $P_{3,1} = -4.7$; $P_{3,3} = 134.8$; $D_{3,3} = 1.9$; $D_{3,5} = -4.0$) as the fixed $I = 3/2$ phase shifts, a total of 114 random sets was introduced. Four distinct solutions were found to be acceptable fits to the π^--p DCS data. These four solutions, after having been fitted with PIPANAL 1CF4, were as shown in Table IX. The π^--p recoil-proton polarization predicted by these four solutions is shown in Fig. 1. It is obvious from the figure that solutions (1) and (2) are in agreement with the data, while (3) and (4) are not. Inclusion of polarization data in the program causes solution (3) to degenerate into solution (1), while the M value of solution (4) increases to a very unacceptable 450 (where 48 is expected).

As is also clear from Fig. 1, polarization data in the region we have explored are quite incapable of resolving solutions (1) and (2). One method of resolving this ambiguity would be to obtain π^--p polarization data at smaller angles. Such data do not exist at present, but an attempt has been made to resolve the two solutions by the inclusion of $\pi^- + p \rightarrow \pi^0 + n$ DCS data.[5] This procedure was

suggested by the large variation in the backward direction of the predicted charge-exchange DCS curves shown in Fig. 2.

Inclusion of the coefficients of Table VIII, together with the polarization data of Table VII, in the search program, yielded the results shown in Table X. Evidently, only solution (1) of Table X now has a reasonable M value, and is therefore considered the only satisfactory spd solution to all the aforementioned data.

2. Yang 3/2 starting point.

While the most intensive work has been centered around the Fermi solution, the Yang spd solution of Foote[7] is perhaps reasonable enough to merit some consideration. We therefore did a considerably smaller amount of random searching in this area also, using as fixed input 3/2 shifts: $S_{3,1} = -23.2$; $P_{3,1} = 126.2$; $P_{3,3} = 159.0$; $D_{3,3} = 7.5$; and $D_{3,5} = -4.6$. In 40 random sets only one solution of $M \leq 50$ ($M = 23$ is expected) appeared; but this solution can be ruled out by π^--p polarization data.

B. spdf Analysis

The same general procedure was followed for the spdf analysis as for the spd analysis. In this case, the Fermi I and Fermi II spdf solutions of Foote[7] were regarded as the most important, and the remaining solutions were treated somewhat more sketchily. "Random" sets were random only in s-, p-, and d-wave phase shifts, with the f waves assumed small and started at zero deg in all cases. However, the final solutions often yielded f-wave phase shifts as large as 10 deg, leading us to believe that no great bias was introduced by starting the f-wave phase shifts at zero.

1. Fermi I and II

Fitting the π^--p DCS data with $I = 3/2$ phase shifts fixed yielded, as one might expect, a considerable number of satisfactory solutions. A total of 450 random sets was run, with a total of 23 good solutions emerging. Of these, 14 were of the Fermi I type and 9 were of the Fermi II type. These sets all gave good fits to the DCS data (see Fig. 3).

Addition of π^--p polarization reduced this number of solutions to 5; these are presented in Table XI. Use of the five charge-exchange DCS coefficients of Caris[5] eliminated solutions (4) and (5). The remaining three are shown in Table XII, and these three solutions are sufficiently different to warrant short individual discussions:

Solution (1) – This is the spdf counterpart of the only good spd solution given in Table X. The $I = 3/2$ phase shifts of the final solution agree very well with Foote's Fermi I solution.[7] Each type of data is individually fitted well. The M value is very close to the expected value; it is the most frequently occurring solution, having appeared 37 times during the random search.

Solution (2) – Although the search yielding this solution began with the $I = 3/2$ phase shifts being fixed at the Fermi I values, the final solution demonstrates a definite Fermi II behavior (i.e., $D_{3,3} - D_{3,5} < 0$). The $I = 3/2$ phase shifts are very different from the Fermi II solution of Foote, but the fit to the π^+-p data is nevertheless quite good. The π^--p polarization data is fitted rather badly, as seen from Fig. 4; however, the fit to the remaining data is sufficiently good that the large contribution to M of the π^--p polarization data (≈ 10) is insufficient to rule out the solution.

Solution (3) – This is a somewhat poorer fit to the data, but still does not possess a sufficiently high M value to be completely ruled out. The I = 3/2 phase shifts are of the Fermi I type, but are not nearly as consistent with the Foote solution as are those of solution (1). Each phase shift does, however, lie within the quoted uncertainty of the Foote solution.[7]

It should be noted that, although the Fermi II solution of Foote was used as a starting point for 200 random sets, it was not possible to find any solution that adequately fitted all the π-p data. Thus it can be concluded that Foote's Fermi II solution can not be used to fit π^--p and π^+-p data simultaneously.

2. Other I = 3/2 starting points

As in the case of the spd analyses, a limited amount of searching was done in which the less-likely I = 3/2 solutions (see Foote's Table VI)[7] were used as starting points. The two solutions treated were the Yang II set and solution No. 6, which is unnamed in the above reference (Foote) and so is here referred to as Fermi Ia. About 100 random cases were examined, with no satisfactory solutions to π^+-p and π^--p (DCS and polarization) appearing.

C. Error Analysis

The matrix-inversion error routine described in Section III-B was applied to the spd solution as well as the three spdf solutions.

1. Error matrices

The error matrices for the four solutions discussed above are tabulated in Appendix A. It is seen that in the spd solution, all rms errors are from 0.3 to 0.9 deg. The correlation coefficients are all relatively small. For the spdf solutions, the errors are considerably larger and the correlation coefficients have also increased in size. The quoted errors on the I = 3/2 phase shift are seen to be similar to those quoted by Foote,[7] indicating that the inclusion of π^--p data has a negligible effect on the I = 3/2 phase-shift error.

D. Inelastic Parameters

To determine the effect of inelastic parameters on the phase shifts, an inelastic I = 1/2 total cross section of $\sigma_I = 0.9 \pm 0.2$ mb[6] was included in the search program, and the inelastic parameters allowed to vary. Only the four final solutions were examined, the results being given in Table XII. In all cases, the inelastic parameters were started at 1.0, although starting them at 0.95 and 0.90 yielded essentially the same results.

V. DISCUSSION OF RESULTS

The analysis of the 310-MeV scattering data in terms of phase shifts has been successful at the d wave level, although 66 pieces of experimental data were needed to eliminate all but one solution. The inclusion of f waves, however, complicates matters considerably.

Perhaps the most disturbing aspect of the spdf wave analysis is the fact that, although the f waves are small in all the satisfactory solutions, the presence of even these very small f waves is seen to radically change the magnitude, and in some cases also the sign, of the phase shifts of the lower orbital-angular-momentum states. This casts doubt on the very premise on which phase-shift analysis is based, i.e., that one can approximate the infinite series that represents the scattering amplitudes by the first few terms. It seems to indicate that the remaining terms in the expansion, although minute in themselves, can nevertheless exert a considerable influence on the larger terms.

A major limitation of the data that now exist at 310 MeV is the very limited angular region of the polarization data, both in π^+-p and π^--p. Especially in π^--p, it would be very instructive to push toward smaller c.m. angles in an attempt to determine the value of polarization at θ near 90 deg. Some attempts have been

made to measure polarization of the recoil proton in the region θ_{cm}=30 to 60 deg, but no data exist at present. A recent preliminary experiment by Booth et al.[16] indicates also the possibility of measuring recoil-neutron polarization in the reaction $\pi^- + p \rightarrow \pi^0 + n$; this measurement, also in the 30 to 60 deg region, would be useful as well in resolving ambiguities between solutions. Developments in polarized targets may in the future make it possible to measure additional quantities corresponding to the triple-scattering parameters in nucleon-nucleon scattering.[17] This would give information on $\mathrm{Im}(g^* h)$, and hence yield another independent experimental quantity.

There is theoretical as well as experimental help that might be utilized. It is hoped that a theoretical approach along the lines used in nucleon-nucleon scattering[18] will be developed, and that accurate predictions of the higher angular momentum phase shifts can be made. Chew et al. have used relativistic dispersion relations to make predictions of the $I = 3/2$ and $1/2$ pion-nucleon d-wave phase shifts up to about 300 MeV.[19] These calculations do not contain possible pion-pion interaction effects and so may not describe these phase shifts accurately. Although some of the d phase shifts in our solutions do agree with these predictions in sign, the agreement in magnitude is not good, and in fact, some of our solutions do not even agree in sign. It is felt that such disagreement should not be taken too seriously until possible π-π effects can be included in the calculation.

Theoretical predictions of the real part of the forward scattering, $\mathrm{Re}[g(0\ \mathrm{deg})]$, using dispersion relations, have been made by Spearman for π^+-p and π^--p scattering.[20] The values quoted here were for the choice $f^2 = 0.08$, where f^2 is the renormalized, unrationalized, pion-nucleon coupling constant.

For π^+-p, Spearman finds

$$\mathrm{Re}[\,g(0\ \mathrm{deg})] \approx -\,0.69,$$

and for π^--p,

$$\mathrm{Re}[\,g(0\ \mathrm{deg})] \approx -\,0.06,$$

in units of $\hbar/\mu c$, where μ denotes the pion rest mass.

The values of Re[g(0 deg)] for π^+-p and π^--p scattering for the d-wave solution (see Table X) and for the three f-wave solutions (see Table XII) are given in Table XIV.

It appears that, at present, no theoretical or experimental data exist that can resolve the ambiguities in the spdf analysis. However, some progress has been made in the knowledge of the phase shifts at 310 MeV. Previously, there was no accurate information about the $I = 1/2$ phase shifts at the energy, but now a choice of three individually accurate sets of phase shifts is available. Also, one $I = 3/2$ solution found by Foote (Fermi II in his notation)[7] was discarded as incapable of fitting all the data adequately. The basic difficulty brought forth by the analysis is the need for very large amounts of experimental data if accurate information about the phase shifts is desired when d, f, and higher partial waves become important. At 310 MeV the inelastic scattering did not add a serious complication. However, because of the sharp increase in inelastic cross section with energy near 300 MeV,[21] phase-shift analysis at slightly higher energies will become even more complicated, since appreciable inelastic scattering essentially doubles the number of parameters that must be determined in the analysis. It appears that because of these requirements for very large amounts of data, the method of phase-shift analysis became less useful at these energies than it had been at lower energies. Eventually, more interest may center on the experimental data themselves and less on the results of the present method of analysis of those data.

ACKNOWLEDGMENTS

It is a pleasure to acknowledge the support of Professor Emilio Segrè. We would like to thank Dr. James Foote for his advice and many helpful discussions. Thanks are also due Mr. David Jenkins for able assistance with tedious hand calculations and many of the programming chores.

APPENDIX: Error matrices

Matrix I. Error matrix for spd solution (expressed in deg^2).

	$S_{3,1}$	$P_{3,1}$	$P_{3,3}$	$D_{3,3}$	$D_{3,5}$	$S_{1,1}$	$P_{1,1}$	$P_{1,3}$	$D_{1,3}$	$D_{1,5}$
$S_{3,1}$	0.4	0.2	0.2	0.1	-0.2	-0.2	-0.2	-0.0	-0.1	0.1
$P_{3,1}$		0.3	0.1	0.1	-0.2	-0.1	-0.2	-0.0	-0.0	0.1
$P_{3,3}$			0.4	0.0	0.0	0.0	-0.1	0.2	-0.1	0.2
$D_{3,3}$				0.1	-0.1	-0.1	-0.0	-0.0	0.0	0.0
$D_{3,5}$					0.2	0.1	0.1	0.1	0.0	-0.0
$S_{1,1}$						0.4	0.0	0.5	0.0	0.1
$P_{1,1}$							0.2	-0.1	0.1	-0.2
$P_{1,3}$								0.8	-0.1	0.3
$D_{1,3}$									0.1	-0.1
$D_{1,5}$										0.4

Matrix II. Error matrix for spdf solution I (expressedin deg^2).

	$S_{3,1}$	$P_{3,1}$	$P_{3,3}$	$D_{3,3}$	$D_{3,5}$	$F_{3,5}$	$F_{3,7}$	$S_{1,1}$	$P_{1,1}$	$P_{1,3}$	$D_{1,3}$	$D_{1,5}$	$F_{1,5}$	$F_{1,7}$
$S_{3,1}$	3.2	3.3	0.5	1.5	-1.7	-0.0	-0.9	-1.5	-1.3	-1.5	-0.2	-0.1	0.0	0.7
$P_{3,1}$		3.8	0.4	1.8	-1.9	-0.0	-1.1	-1.7	-1.4	-1.7	-0.2	-0.3	0.1	0.8
$P_{3,3}$			0.4	0.1	-0.1	0.0	-0.1	-0.2	-0.3	-0.0	-0.1	0.2	0.0	0.1
$D_{3,3}$				0.9	-0.9	0.0	-0.5	-0.8	-0.6	-0.8	-0.1	-0.2	0.0	0.3
$D_{3,5}$					1.0	0.0	0.5	0.9	0.7	0.9	0.1	0.2	-0.0	-0.4
$F_{3,5}$						0.1	-0.0	-0.0	-0.0	-0.0	-0.0	-0.0	-0.0	-0.0
$F_{3,7}$							0.3	0.5	0.4	0.5	0.1	0.1	-0.0	-0.2
$S_{1,1}$								2.2	0.6	1.3	0.3	0.5	-0.2	0.3
$P_{1,1}$									0.7	0.5	-0.2	-0.1	0.0	-0.3
$P_{1,3}$										1.7	-0.0	0.6	-0.0	-0.3
$D_{1,3}$											0.1	-0.1	-0.0	0.1
$D_{1,5}$												0.6	-0.0	0.1
$F_{1,5}$													0.1	-0.1
$F_{1,7}$														0.5

Matrix III. Error matrix for spdf solution II (expressed in deg^2).

	$S_{3,1}$	$P_{3,1}$	$P_{3,3}$	$D_{3,3}$	$D_{3,5}$	$F_{3,5}$	$F_{3,7}$	$S_{1,1}$	$P_{1,1}$	$P_{1,3}$	$D_{1,3}$	$D_{1,5}$	$F_{1,5}$	$F_{1,7}$
$S_{3,1}$	0.2	0.1	0.1	0.1	-0.1	0.0	-0.0	0.2	0.1	0.0	0.0	0.0	-0.0	-0.0
$P_{3,1}$		0.7	-0.4	0.5	-0.6	0.3	-0.3	-0.2	-0.2	-0.2	-0.2	0.3	-0.1	0.1
$P_{3,3}$			0.7	-0.3	0.5	-0.2	0.2	0.2	0.4	-0.1	0.2	-0.2	0.1	-0.1
$D_{3,3}$				0.4	-0.4	0.2	-0.2	0.1	-0.1	0.1	-0.2	0.2	-0.1	0.1
$D_{3,5}$					0.6	-0.2	0.3	-0.1	0.1	-0.1	0.2	-0.3	0.1	-0.1
$F_{3,5}$						0.2	-0.1	0.1	-0.1	0.1	-0.1	0.1	-0.1	0.1
$F_{3,7}$							0.2	-0.1	0.1	-0.1	0.1	-0.1	0.1	-0.1
$S_{1,1}$								1.8	0.7	0.4	0.1	0.1	-0.1	0.1
$P_{1,1}$									0.9	0.1	0.3	0.1	0.1	-0.0
$P_{1,3}$										0.5	0.0	0.2	-0.0	0.1
$D_{1,3}$											0.2	-0.0	0.1	-0.0
$D_{1,5}$												0.3	-0.2	0.1
$F_{1,5}$													0.1	-0.1
$F_{1,7}$														0.1

Matrix IV. Error matrix for spdf solution III (expressed in deg^2).

	$S_{3,1}$	$P_{3,1}$	$P_{3,3}$	$D_{3,3}$	$D_{3,5}$	$F_{3,5}$	$F_{3,7}$	$S_{1,1}$	$P_{1,1}$	$P_{1,3}$	$D_{1,3}$	$D_{1,5}$	$F_{1,5}$	$F_{1,7}$
$S_{3,1}$	1.9	2.2	0.2	1.2	-1.1	0.2	-0.7	0.4	-0.7	0.8	-0.6	0.6	-0.1	0.4
$P_{3,1}$		3.0	0.1	1.7	-1.4	0.2	-0.9	0.4	-1.1	1.1	-0.8	0.7	-0.1	0.6
$P_{3,3}$			0.4	0.0	0.0	0.0	-0.0	0.2	0.3	0.2	-0.0	0.0	0.0	0.0
$D_{3,3}$				1.1	-0.8	0.1	-0.6	0.2	-0.7	0.6	-0.5	0.4	-0.1	0.3
$D_{3,5}$					0.8	-0.1	0.4	-0.2	0.6	-0.5	0.4	-0.4	0.1	-0.3
$F_{3,5}$						0.1	-0.1	0.0	-0.1	0.1	0.1	0.0	-0.0	0.0
$F_{3,7}$							0.3	-0.1	0.4	-0.3	0.2	-0.2	0.0	-0.2
$S_{1,1}$								1.9	0.2	1.0	-0.7	0.4	-0.4	0.0
$P_{1,1}$									1.6	-0.6	0.4	-0.3	0.2	-0.2
$P_{1,3}$										1.0	-0.5	0.5	-0.3	0.2
$D_{1,3}$											0.6	-0.2	0.1	-0.1
$D_{1,5}$												0.3	-0.1	0.2
$F_{1,5}$													0.2	0.0
$F_{1,7}$														0.1

*Work done under the auspices of the U.S. Atomic Energy Commission.

†Present address: Lawrence Radiation Laboratory, University of California, Livermore, California.

‡Present address: Aerospace Corporation, Los Angeles, California.

1. E. H. Rogers, O. Chamberlain, J. Foote, H. Steiner, C. Wiegand, and T. Ypsilantis, Rev. Mod. Phys. 33, 356 (1961).
2. J. Foote, O. Chamberlain, E. Rogers, H. Steiner, C. Wiegand, and T. Ypsilantis, Phys. Rev. 122, 948 (1961).
3. H. R. Rugge and O. T. Vik (preceding paper). This paper is the second of a series of two: the first was entitled "π^--p Elastic Scattering at 310 MeV: Differential Cross-Section and Recoil-Proton Polarization." (Submitted to Phys. Rev.).
4. H. R. Rugge, Scattering of Negative Pions on Protons at 310 MeV: Differential and Total Cross-Sections and Phase-Shift Analysis, (Ph.D. Thesis), Lawrence Radiation Laboratory Report UCRL-10252, May 1962 (unpublished).
5. J. C. Caris, R. W. Kenney, V. Perez-Mendez, and W. A. Perkins, Phys. Rev. 121, 893 (1961).
6. B. C. Barish, R. Kurz and J. Solomon (private communication).
7. J. Foote, O. Chamberlain, E. Rogers, and H. Steiner, Phys. Rev. 122, 959 (1961).
8. H. A. Bethe and P. Morrison, Elementary Nuclear Theory, 2nd Ed. (John Wiley and Sons, Inc., New York, 1956), pp. 133-142.
9. J. Ashkin, Nuovo Cimento Suppl. 14, 221 (1959).
10. H. A. Bethe and F. de Hoffmann, Mesons and Fields (Row, Peterson and Company, Evanston, Illinois, 1955), Vol. II.

11. H. P. Stapp, T. J. Ypsilantis, and N. Metropolis, Phys. Rev. 105, 302 (1957).

12. Frank T. Solmitz, Phys. Rev. 94, 1799 (1954).

13. E. Fermi, N. Metropolis, and E. F. Alei, Phys. Rev. 95, 1581 (1954).

14. H. L. Anderson, E. Fermi, R. Martin and D. E. Nagle, Phys. Rev. 91, 155 (1953).

15. A more detailed account of this work can be found in Olav T. Vik, Scattering of Negative Pions on Protons at 310 MeV: Recoil-Nucleon Polarization and Phase-Shift Analysis (Ph. D. Thesis), Lawrence Radiation Laboratory Report UCRL-10253, May 1962 (unpublished).

16. N. E. Booth, R. Hill, N. H. Lipman, H. R. Rugge, and O. T. Vik, Physics Division Semiannual Report, May through October 1961, Lawrence Radiation Laboratory Report UCRL-10113, March 1962 (unpublished), p. 47.

17. Tom J. Ypsilantis, Experiments on Polarization in Nucleon-Nucleon Scattering at 310 MeV (Ph. D. Thesis), University of California Radiation Laboratory Report UCRL-3047, June 1955 (unpublished).

18. M. MacGregor, M. Moravcsik, and H. P. Noyes, Phys. Rev. 123, 1835 (1961).

19. G. F. Chew, M. Goldberger, F. Low, and Y. Nambu, Phys. Rev. 106, 1337 (1957).

20. T. D. Spearman, Nuovo Cimento 15, 147 (1960).

21. Walton A. Perkins III, Positive Pion Production by Negative Pions (Ph. D. Thesis), Lawrence Radiation Laboratory Report UCRL-8778, June 1959 (unpublished).

Table I. Scattering amplitudes for charged pions and protons.

Reaction	Scattering amplitudes	
	Non-spin-flip	Spin-flip
(a) $\pi^+ + p \rightarrow \pi^+ + p$	$g(I=3/2)$	$h(I=3/2)$
(b) $\pi^- + p \rightarrow \pi^- + p$	$1/3g(I=3/2)+2/3g(I=1/2)$	$1/3h(I=3/2)+2/3h(I=1/2)$
(c) $\pi^- + p \rightarrow \pi^0 + n$	$\frac{\sqrt{2}}{3}[g(I=3/2) - g(I=1/2)]$	$\frac{\sqrt{2}}{3}[h(I=3/2) - h(I=1/2)]$

Table II. Nonrelativistic Coulomb phase shifts, first-order relativistic corrections, and complete Coulomb phase shifts (all in degrees) for incident pion kinetic energy $T = 310$ MeV.

ℓ	Φ_ℓ	$\Delta\Phi_\ell^{+}$	$\Delta\Phi_\ell^{+}$	Φ_ℓ^{+}	Φ_ℓ^{-}
0	0.00	0.09	----	0.09	----
1	0.44	0.09	-0.17	0.53	0.27
2	0.66	0.06	-0.09	0.72	0.57
3	0.81	0.04	-0.06	0.95	0.75

Table III. Phase-shift symbols.

ℓ	J	Phase-shift symbol	
		I=3/2	I=1/2
0	1/2	$S_{3,1}$	$S_{1,1}$
1	1/2	$P_{3,1}$	$P_{1,1}$
1	3/2	$P_{3,3}$	$P_{1,3}$
2	3/2	$D_{3,3}$	$D_{1,3}$
2	5/2	$D_{3,5}$	$D_{1,5}$
3	5/2	$F_{3,5}$	$F_{1,5}$
3	7/2	$F_{3,7}$	$F_{1,7}$

Table IV. Differential and total cross section[a] for $\pi^- + p \rightarrow \pi^- + p$ at 310 MeV.

θ_{cm} (deg)	$\frac{d\sigma(\theta)}{d\Omega_{cm}}$ (mb/sr)	rms uncertainty (mb/sr)
34.7	1.184	0.043
41.4	1.171	0.035
47.9	1.151	0.033
54.4	1.125	0.029
60.6	1.027	0.027
66.8	0.970	0.023
72.7	0.853	0.023
78.5	0.774	0.018
84.1	0.690	0.018
89.6	0.635	0.015
94.9	0.561	0.017
100.0	0.498	0.013
105.0	0.461	0.014
109.8	0.480	0.009
114.5	0.482	0.016
119.0	0.514	0.012
123.5	0.536	0.013
127.8	0.590	0.018
132.0	0.663	0.016
136.0	0.715	0.016
140.0	0.764	0.021
144.0	0.822	0.020
147.8	0.817	0.021
151.6	0.889	0.025
155.2	0.941	0.015
158.9	0.991	0.028
162.4	0.932	0.029
166.0	0.944	0.042

[a]The total cross section used in the analysis was 28.8±0.8 mb, evaluated between c.m. cutoff angles 8.4 and 167.4 deg. The normalization uncertainty (see Section III-B) was taken to be $\Delta\epsilon = 0.03$.

Table V. Differential and total cross section[a] for $\pi^+ + p \rightarrow \pi^+ + p$ at 310 MeV, measured by Rogers.[b]

θ_{cm} (deg)	$\frac{d\sigma(\theta)}{d\Omega_{cm}}$ (mb/sr)	rms uncertainty (mb/sr)
14.0	18.71	0.60
19.6	16.05	0.46
25.2	13.82	0.31
30.6	12.99	0.25
34.6	12.28	0.27
36.2	11.65	0.27
44.0	9.82	0.15
51.8	8.59	0.26
56.8	7.54	0.28
60.0	6.58	0.22
69.6	4.73	0.10
75.3	3.62	0.09
81.6	2.77	0.08
97.8	1.66	0.07
105.0	1.51	0.06
108.1	1.62	0.07
120.9	2.08	0.08
135.2	2.93	0.14
140.6	3.36	0.12
144.7	3.76	0.15
152.2	4.10	0.21
156.4	4.51	0.17
165.0	4.88	0.12

[a]The total cross section used in the analysis was 56.4±1.4 mb, evaluated between c.m. cutoff angles 14.7 and 158.0 deg. The normalization uncertainty (see Section III-B) was taken to be $\Delta\epsilon = 0.06$.

[b]See reference 1.

Table VI. Recoil-proton polarization for $\pi^+ + p \rightarrow \pi^+ + p$ at 310 MeV, measured by Foote.[a]

θ_{cm} (deg)	$P(\theta)$	rms uncertainty (mb/sr)
114.2	0.044	0.062
124.5	-0.164	0.070
133.8	-0.155	0.044
145.2	-0.162	0.037

[a]See reference 2.

Table VII. Recoil-proton polarization for $\pi^- + p \rightarrow \pi^- + p$ at 310 MeV.

θ_{cm} (deg)	$P(\theta)$	rms uncertainty (mb/sr)
114.2	0.784	0.132
124.5	0.648	0.076
133.8	0.589	0.072
145.2	0.304	0.055

Table VIII. Coefficients for Legendre polynomial fit to $\pi^- + p \rightarrow \pi^0 + n$ DCS, measured by Caris at 317 MeV.[a]

$$\frac{d\sigma(\theta)}{d\Omega_{cm}} = \sum_{\ell=1}^{\ell_{max}} A_\ell \, P_\ell(\cos\theta)$$

	Coefficient (mb/sr)	rms uncertainty[b] (mb/sr)
A_1	1.39	0.06
A_2	1.87	0.11
A_3	1.50	0.17
A_4	0.01	0.15
A_5	-0.35	0.42

[a]See reference 5.

[b]The normalization uncertainty (see Section III-B) was taken to be $\Delta\epsilon = 0.10$.

Table IX. spd solutions to π^--p DCS and total cross-section data (also π^+-p DCS, polarization, and total cross-section data).

	$M_{expected}=47^a$	$S_{3,1}$	$P_{3,1}$	$P_{3,3}$	$D_{3,3}$	$D_{3,5}$	$S_{1,1}$	$P_{1,1}$	$P_{1,3}$	$D_{1,3}$	$D_{1,5}$
(1)	52.4	-18.8	-5.0	134.9	1.7	-3.7	-5.8	-4.0	4.4	-5.3	15.1
(2)	61.3	-18.2	-4.5	135.1	1.9	-4.0	-7.2	25.8	27.3	73.0	-0.5
(3)	57.8	-18.5	-4.7	134.7	1.9	-4.0	24.2	10.5	-2.0	3.6	-0.0
(4)	52.1	-18.9	-5.0	134.3	1.8	-3.9	-4.0	-0.6	5.3	17.3	1.0

Table X. spd solutions to π^--p DCS, polarization, total cross-section and charge-exchange coefficients (also π^+-p DCS, polarization, and total cross-section data)

	$M_{expected}$=56[a]	$S_{3,1}$	$P_{3,1}$	$P_{3,3}$	$D_{3,3}$	$D_{3,5}$	$S_{1,1}$	$P_{1,1}$	$P_{1,3}$	$D_{1,3}$	$D_{1,5}$
(1)	71.2	-18.8	-4.9	135.5	1.7	-3.6	-6.2	-4.0	3.9	-5.5	15.2
(2)	123.4	-18.3	-4.4	135.7	1.8	-3.9	-2.6	28.7	6.7	2.8	-0.3

[a] $M_{expected}$ means the number of degrees of freedom, i.e., (number of experimental points fitted) minus (number of phase shifts varied).

Table XI. spdf Solutions to π^+-p and π^--p DCS, polarization, and total cross section.

$M_{expected} = 47^a$

	M	Started from	$S_{3,1}$	$P_{3,1}$	$P_{3,3}$	$D_{3,3}$	$D_{3,5}$	$F_{3,5}$	$F_{3,7}$	$S_{1,1}$	$P_{1,1}$	$P_{1,3}$	$D_{1,3}$	$D_{1,5}$	$F_{1,5}$	$F_{1,7}$
I	37.9	Fermi I	-15.3	-0.0	134.8	4.8	-6.4	0.8	-1.6	-5.4	-5.3	2.0	-5.5	15.9	-0.2	2.4
II	48.3	"	-20.7	-10.1	136.1	-2.0	-0.3	-1.1	2.3	11.7	23.4	-2.0	6.7	2.5	2.2	-0.4
III	41.3	"	-15.1	0.1	135.0	4.9	-6.4	0.8	-1.7	-0.2	27.2	7.3	-0.3	-1.6	-2.5	-0.2
IV	49.1	"	-17.4	-2.8	134.2	3.2	-5.1	0.6	-0.8	10.3	20.2	-1.2	5.3	5.7	1.8	0.8
V	46.6	Fermi II	-35.5	-16.0	151.3	-11.4	13.0	-1.1	-1.9	-13.0	3.7	19.7	-0.6	-2.0	2.5	1.0

Table XII. spdf Solutions to π^+-p and π^--p DCS, polarization, total cross section, and π^--p $\rightarrow \pi^0$n DCS.

$M_{expected} = 52$[a]

	M	$S_{3,1}$	$P_{3,1}$	$P_{3,3}$	$D_{3,3}$	$D_{3,5}$	$F_{3,5}$	$F_{3,7}$	$S_{1,1}$	$P_{1,1}$	$P_{1,3}$	$D_{1,3}$	$D_{1,5}$	$F_{1,5}$	$F_{1,7}$
I	43.7	-14.4	1.1	135.1	5.4	-6.9	0.8	-2.0	-6.0	-5.8	1.5	-5.7	15.8	-0.2	2.5
II	64.2	-21.2	-12.1	137.2	-3.3	1.5	-1.8	3.3	10.9	23.1	-3.5	6.5	0.6	2.1	-1.2
III	71.7	-15.6	-0.7	135.3	4.2	-6.0	0.7	-1.3	5.0	27.9	9.2	-0.5	-0.7	-3.2	-0.5

[a] $M_{expected}$ means the number of degrees of freedom, i.e., (number of experimental points fitted) minus (number of phase shifts varied).

Table XIII. spd and spdf solutions including the inelastic total cross section.

	spd solution				
	$S_{3,1}$	$P_{3,1}$	$P_{3,3}$	$D_{3,3}$	$D_{3,5}$
I = 3/2					
phase shifts	-18.9	-5.0	135.5	1.6	-3.4
	$S_{1,1}$	$P_{1,1}$	$P_{1,3}$	$D_{1,3}$	$D_{1,5}$
I = 1/2					
phase shifts	-6.0	-3.9	4.0	-5.3	14.9
Corresponding inelastic parameters[a]	0.98	1.00	1.00	0.99	1.00

	spdf solution I						
	$S_{3,1}$	$P_{3,1}$	$P_{3,3}$	$D_{3,3}$	$D_{3,5}$	$F_{3,5}$	$F_{3,7}$
I = 3/2							
phase shifts	-14.9	0.4	135.1	5.1	-6.5	0.8	-1.8
	$S_{1,1}$	$P_{1,1}$	$P_{1,3}$	$D_{1,3}$	$D_{1,5}$	$F_{1,5}$	$F_{1,7}$
I = 1/2							
phase shifts	-5.9	-5.5	1.7	-5.5	15.3	-0.1	2.3
Corresponding inelastic parameters	1.00	1.00	0.99	0.99	1.00	1.00	1.00

Table XIII. spd and spdf solutions including the inelastic total cross section. (continued)

	spdf solution II						
	$S_{3,1}$	$P_{3,1}$[a]	$P_{3,3}$	$D_{3,3}$	$D_{3,5}$	$F_{3,5}$	$F_{3,7}$
I = 3/2							
phase shifts	-21.1	-11.8	137.0	-3.1	1.2	-1.7	3.1
	$S_{1,1}$	$P_{1,1}$	$P_{1,3}$	$D_{1,3}$	$D_{1,5}$	$F_{1,5}$	$F_{1,7}$
I = 1/2							
phase shifts	10.9	23.0	-3.6	5.9	0.3	1.8	-0.7
Corresponding inelastic parameters	1.00	0.94	1.00	1.00	1.00	1.00	1.00

	spdf solution III						
	$S_{3,1}$	$P_{3,1}$	$P_{3,3}$	$D_{3,3}$	$D_{3,5}$	$F_{3,5}$	$F_{3,7}$
I = 3/2							
phase shifts	-15.4	-0.4	135.6	4.4	-6.2	0.7	-1.4
	$S_{1,1}$	$P_{1,1}$	$P_{1,3}$	$D_{1,3}$	$D_{1,5}$	$F_{1,5}$	$F_{1,7}$
I = 1/2							
phase shifts	3.7	26.4	8.6	-0.3	3.1	-0.6	-0.1
Corresponding inelastic parameters	1.00	1.00	0.98	1.00	1.00	1.00	1.00

[a]See Section IV-D.

Table XIV. Re[g(0 deg)] in units of $\hbar/\mu c$ for π^+-p and π^--p scattering at 310 MeV for d-wave solution and 3 f-wave solutions listed in the text.

Solution	π^--p Re[g(0 deg)]	π^+-p Re[g(0 deg)]
d(1)	-0.08±0.02	-0.69±0.01
f I	-0.04±0.03	-0.68±0.02
f II	-0.01±0.02	-0.69±0.01
f III	-0.06±0.03	-0.69±0.01
Spearman prediction	-0.06	-0.69

LEGENDS

Fig. 1. Recoil-proton polarization in π^--p elastic scattering at 310 MeV. Cases plotted are those d-wave solutions given in Table IX.

Fig. 2. Comparison between predicted and measured charge-exchange DCS. Error flag shows approximate uncertainty in experimental measurement at backward angles.

Fig. 3. The spdf solution (I) fit to π^--p DCS data. The other two spdf solutions give comparable fits to the data.

Fig. 4. Recoil-proton polarization in π^--p elastic scattering at 310 MeV. Cases plotted are those f-wave solutions given in Table XI.

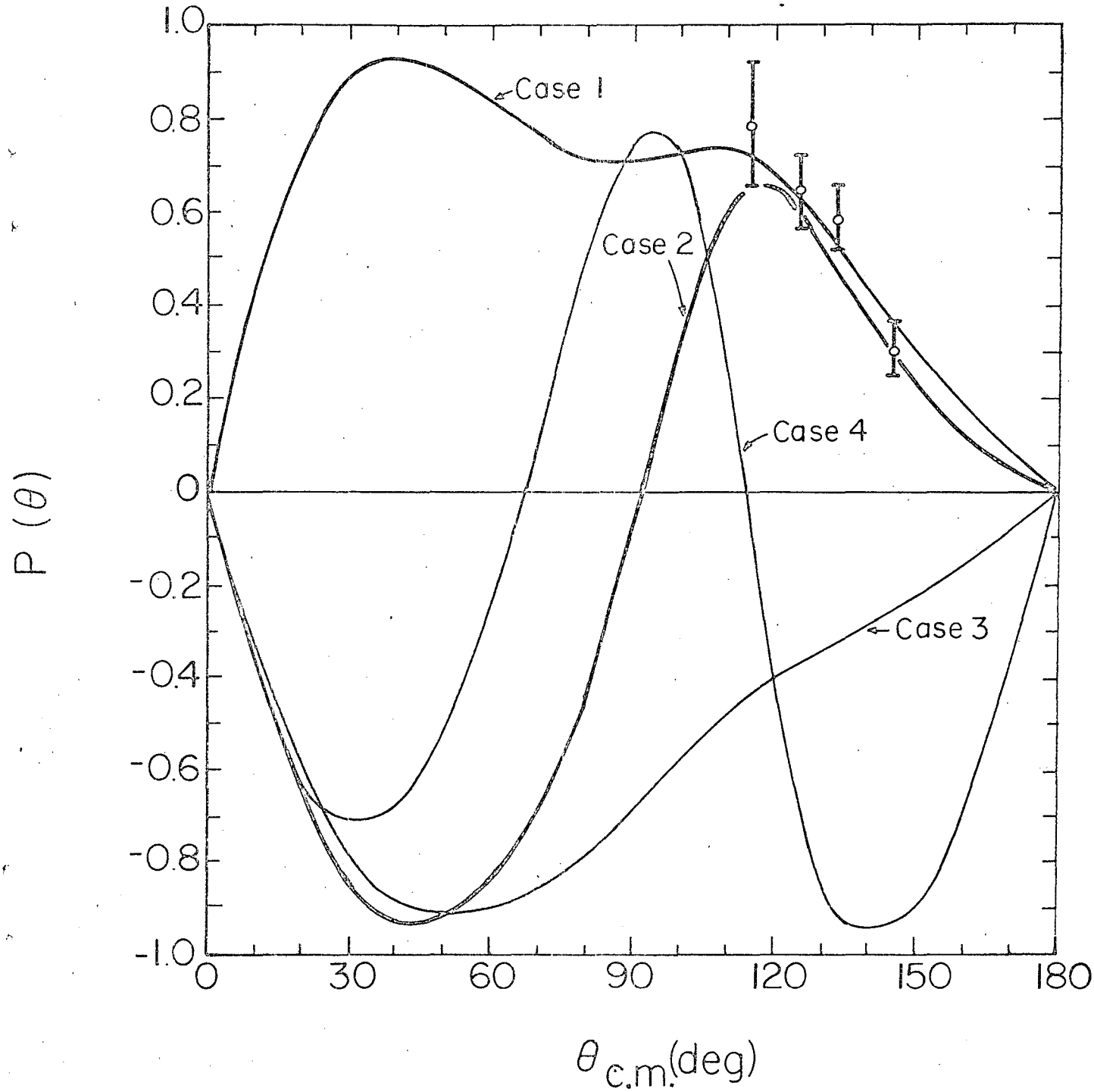

MU-27358

Fig. 1

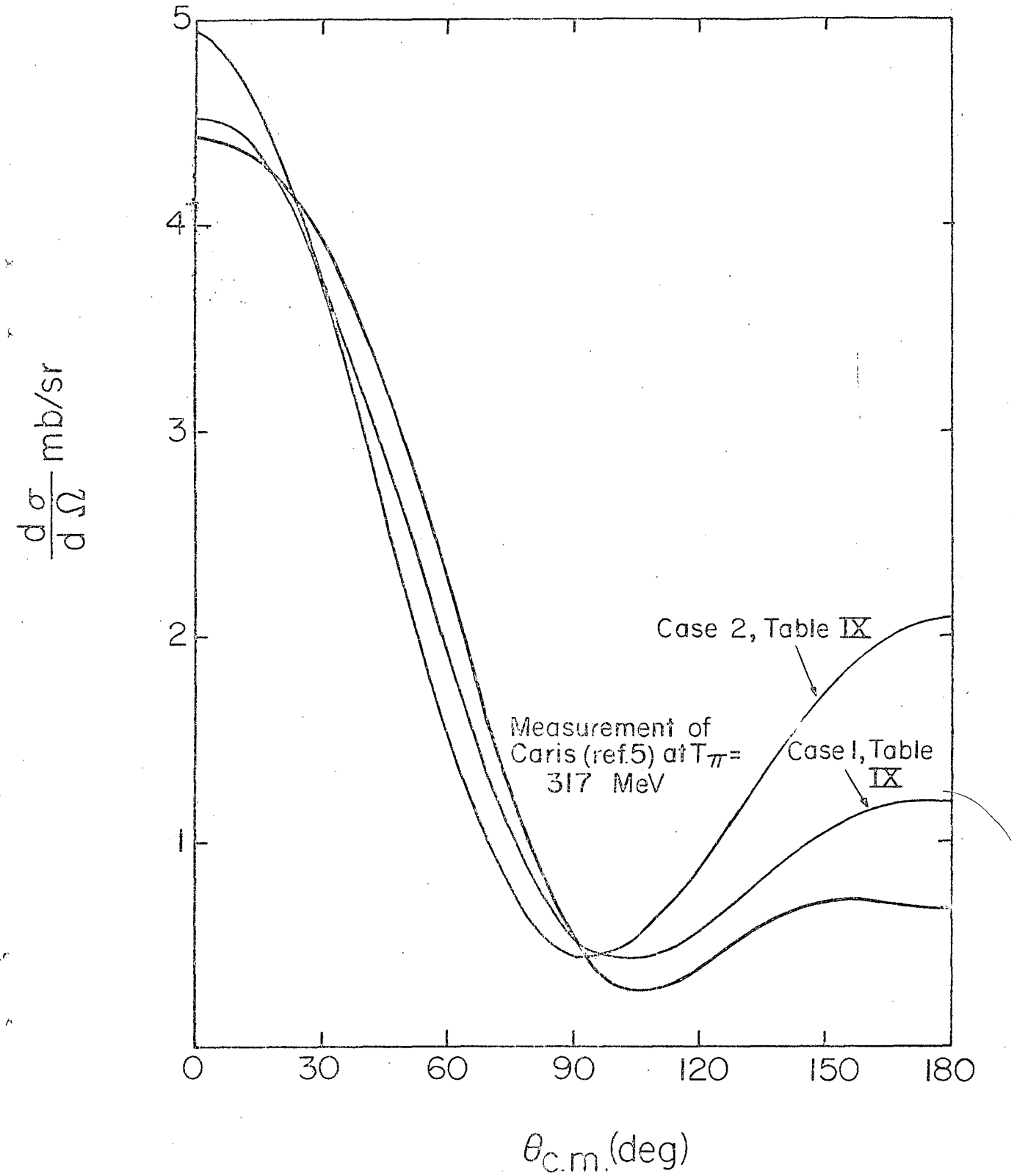

MU-27359

Fig. 2

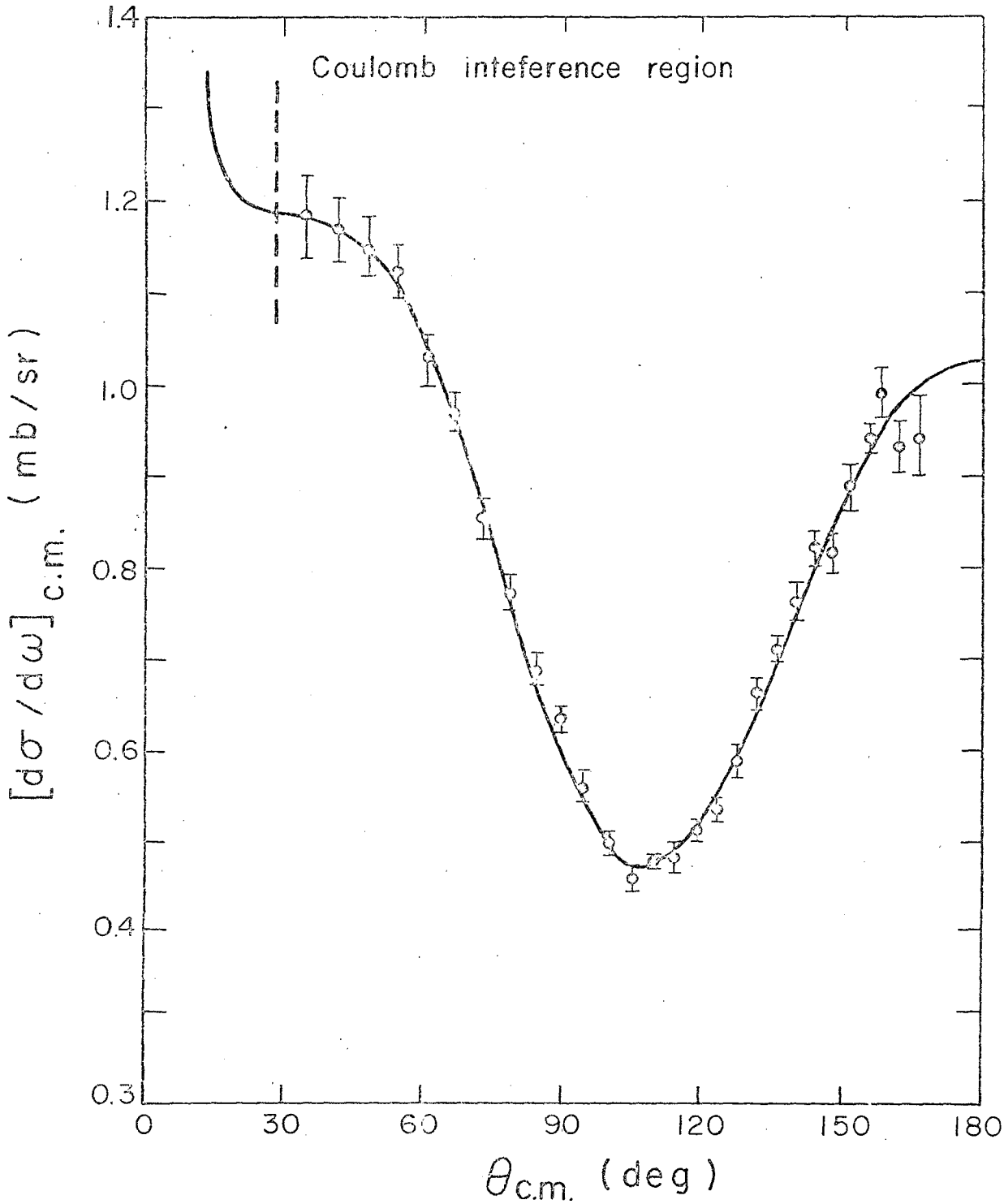

Fig. 3

MU-27121

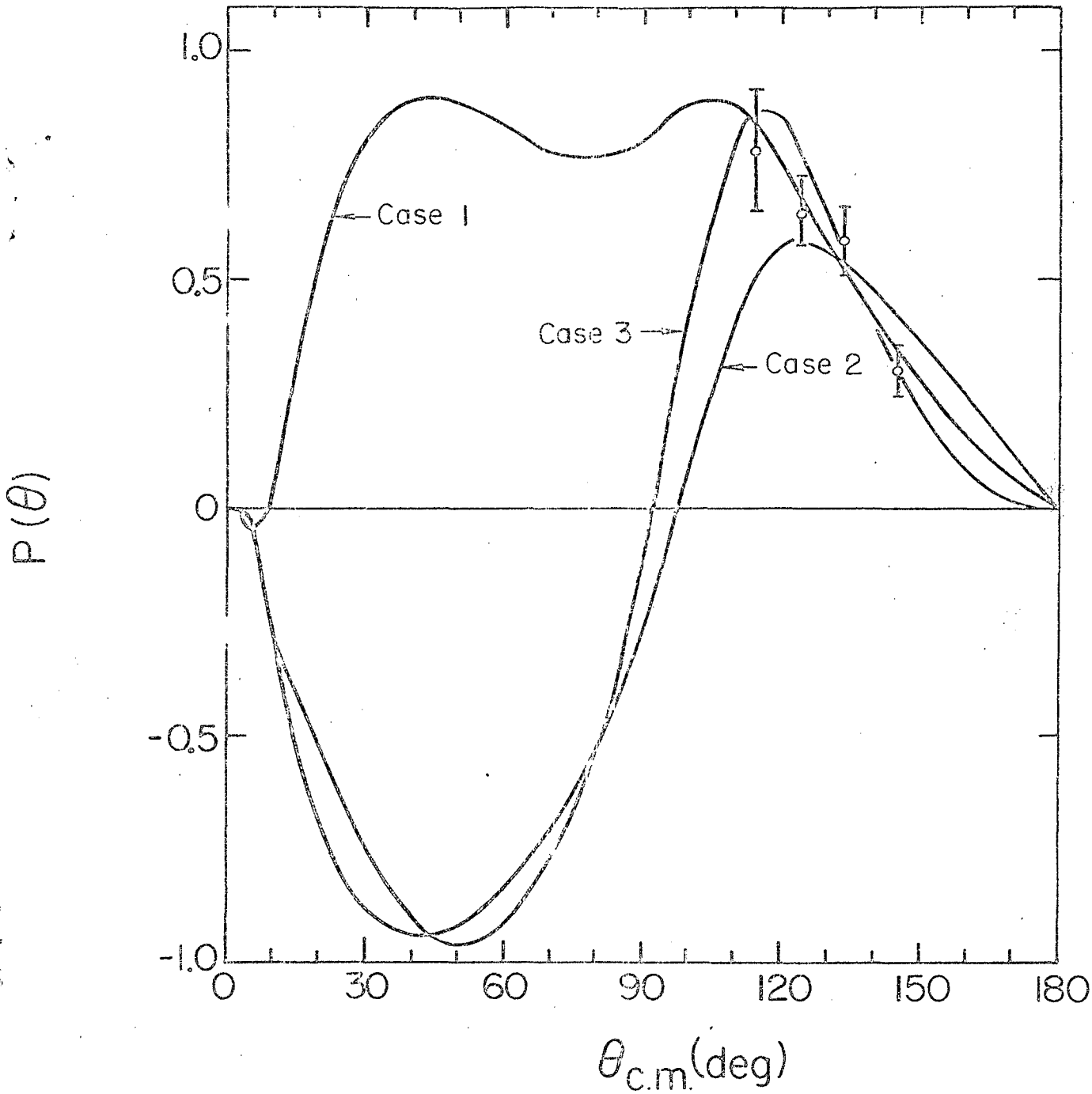

MU-27365

Fig. 4

OCT 15 1962